Cosmic ray primary composition in the energy range 10–1000 TeV obtained by passive balloon-borne detector: Reanalysis of the RUNJOB experiment

V. Kopenkin*
Skobelevskaya st. 42-15, Yuzhnoe Butovo, Moscow, Russia

T. Sinzi
Rikkyo University, Toshima-ku, Tokyo, 171 Japan

(Received 21 February 2008; revised manuscript received 10 March 2009; published 30 April 2009)

We search for a consistent view on the RUNJOB experiment and present an alternative analysis based on explicitly reported and published numerical data. Here we show that there is more than one interpretation to the reported observational data. It is demonstrated that, contrary to the wide-spread opinion, the RUNJOB data are not inconsistent with an increase of the average mass near the knee region of the cosmic ray spectrum. Considering very low statistics and systematic uncertainties, especially in the high energy region, we suggest that peculiarities of the methodical origin were the most likely source of those RUNJOB conclusions which contradicted previous observations reported by other groups.

DOI: 10.1103/PhysRevD.79.072011 PACS numbers: 96.50.sb, 13.85.−t

I. INTRODUCTION

Study of the cosmic ray mass composition in the energy region 10–1000 TeV has been an active field for many years, with various methods and techniques applied. One of the most prominent features in understanding the origin of cosmic rays is the ''knee'' puzzle ($3–4 \times 10^{15}$ eV) of the cosmic ray spectrum. To investigate a relationship between the cosmic ray source spectrum and the knee, one must detect individual elements, measure their spectra, and analyze their spectral differences. For the present status of research in this extremely active area see, for instance, [1]. The RUNJOB (Russia-Nippon-joint-balloon) experiment aimed at ''direct observation of cosmic rays in the knee region'' [2]. In 1995–1999 there were ten successful balloon flights of traditional calorimeter-type emulsion chambers [3] with an area of 0.4 m^2 and weight ~230–260 kg, on the trans-Siberian route at an altitude of ~30 km (10–12 g/cm^2), each time for about a week. The total accumulated exposure was reported as 575 m^2 h [4].

Based on ''eight chambers'' [5] observations (231.5 m^2 h exposition [5]), RUNJOB reported that the proton spectrum is ''nearly consistent with those reported by other groups in the past.'' The helium flux was claimed to be ''nearly half'' [5] of the value previously obtained by JACEE [6]. RUNJOB concluded that the proton and helium spectra show ''almost parallel'' slopes of the spectra (2.7–2.8 in the energy range 10–500 TeV/nucleon), while heavier particles' spectra are ''gradually hardening'' [7] (''2.7 for the CNO group'' and ''~2.6 for Fe'') [4]. The discrepancy with the previous passive balloon-borne experiment (JACEE) was described as ''critical for our understanding of the origin of cosmic rays and the acceleration mechanism'' by supernova in the Galaxy, ''leading to quite different alternatives'' [4,5]. The detection of a single proton event was interpreted as ''the first direct evidence to accelerate a proton to PeV/nucleon energy'' [8]. Some ''flattering in the slope of the spectrum above 100 TeV/particle'' was suggested to be a ''new effect,'' ''for instance some new component, either from our Galaxy or the extra Galaxy'' [8]. The ''full report'' [4] based on ''final results'' [4] stated that ''the RUNJOB data show a constant average mass up to 1 PeV/particle'' [4]. Basically, RUNJOB offered new data in the energy region which has been previously extensively studied by other experiments (JACEE, MUBEE) based on similar passive calorimeter technique [9,10]. The RUNJOB conclusions have caused considerable attention in recent years, particularly among indirect experiments, which heavily rely on primary spectra evaluation [11–16].

The numerous details and information on the RUNJOB data have been extensively presented by RUNJOB at many occasions since the very beginning of the experiment which commenced in 1995 [2]. Based on our previous study of so-called ''exotic events'' observed by emulsion chamber detectors [17,18], in present analysis we search for mundane scenarios that could lead the analysis astray and discuss the RUNJOB data with an eye to what is missing or can be inaccurate with analysis that might distort the reader's conclusions (or data's evaluation). The reanalysis of the RUNJOB data [5] was inspired by several critical comments made by Professor Grigorov in 2001 [19]. After the actual numerical data of the 1995–1996 exposition [5] were published, it was noticed in 2003 that RUNJOB should not withdraw from consideration gamma rays, which are particularly essential for the emulsion chamber method of observation [20]. Subsequently, it was realized that, in order to construct a consistent view on the RUNJOB experiment *itself*, to search for patterns, we must look at the complete data sets (particle tracks and

*vvk20032004@yahoo.com

gamma rays), as they were presented and published. It was demonstrated that the RUNJOB data on gamma rays were at variance with the RUNJOB conclusions based on primary particle tracks [21,22]. It was shown that the observed gamma rays above 10 TeV can be an indication of an increase of heavy primaries [22]. While the analysis was under way, there was startling [23] news that RUNJOB already published a so-called ''final'' report [4]. We believe that the process of reexamination of the published RUNJOB claims, as well as critical assessment of the possibility of experimental, methodological, and human errors at every stage of the experiment, is not less important than a conjecture of some particular acceleration mechanism that could have occurred in a simulated image of a galaxy. In the present paper we make our own evaluation of the RUNJOB data based on publicly available sources. We rely on examination of the explicit numerical data, records, tables, images, and figures. We are focusing on what can be learned from experimental observations with traditional passive instruments that return vast quantities of particle tracks, interpreted mainly by human visual analysis. In the present analysis we are based primarily on RUNJOB 1995–1996 data [24], the only data that were explicitly presented in numerical, tabulated form [5,25]. Our results suggest that the most likely reason that the RUNJOB conclusions were different from previous balloon-borne observations of similar type is that the methods of the experimental signal assessment were constrained by poor accuracy and low statistics. This analysis reminds that standard physics activity always requires independent critical consideration of possible methodological and human errors, particularly at the present time, when new fundamental challenges can be met only by collaborative actions with involvement of significant multinational public resources.

II. EXPERIMENTAL SETUP

Here we present basic general information on the passive balloon-borne experiment RUNJOB. Specific technical details and an overall description of similar passive balloon-borne experiments can be found in their original papers [6,9,10].

A. Emulsion chamber

Basically, the emulsion chamber detector consists of three main parts (called modules, according to the RUNJOB specification [5]): primary layer, target, and calorimeter (see Table I). The primary layer is used for charge determination of incoming particles. The target is for nuclear interactions. The calorimeter is a stack of nuclear emulsions, x-ray films, and lead plates. The spacer (between the target and the calorimeter) enables lateral spread for individual high energy secondary particles originated in the interaction. The vertical thickness of the RUNJOB chamber was $\sim$0.4 of proton mean-free path (MFP), and the calorimeter thickness $\sim$3–5 radiation lengths [5,26]. When a cosmic ray particle of electromagnetic component is produced in the chamber or arrives at the chamber from the outside, it produces an electron shower in the calorimeter part of the chamber. The shower produces a black spot on the x-ray film, the spot darkness is determined by photometry measurements. The darkness of the shower at the maximum of the cascade shower curve is approximately proportional to the shower energy (ΣE_γ).

B. Primary particle identification

Identification of the cosmic ray projectile is made using various kinds of sensitive materials (x-ray emulsions and nuclear emulsion plates). Showers are recorded on x-ray emulsion film as dark spots. These spots are identified by the naked eye for showers with energy larger than $\sim$1 TeV. The detection threshold of spot darkness, D_{th} is ($\sim$ 0.1–0.2), varying with the background darkness and other film conditions. The scanning of shower spots is made generally over all available x-ray films. The detected shower is traced through the chamber. The data set (D, t), where t is the depth of the x-ray layer in the chamber, determines the shower transition curve. A shower trajec-

TABLE I. Chamber structure in 1995–1999 experiments. UC stands for upper calorimeter. LC stands for lower calorimeter. Data are based on [26–28]. The target material in the case of the 1996 chamber was stainless steel plate [5]. Instead of LC, there is a diffuser (D) module in RUNJOB 1997 and RUNJOB 1999. A typical chamber consists of two units. The chamber unit is called block here. The eight chambers mentioned by RUNJOB in [5] correspond to eight blocks in our classification. MFP stands for mean-free path.

Year	Weight kg	Modules Primary mm	Target mm	Spacer mm	UC mm	LC(D) mm	UC + LC c.u.	Thickness Chamber Proton MFP	Chamber Fe MFP
1995	230	4.62	99.82	187.37	57.72	43.41	3.60	0.40[b]	2.44[c]
1996	254[a]	8.85	37.76	53.15	91.00	19.79	4.24	0.35	1.51
1997	260	4.54	47.08	102.72	37.86	37.32	4.43	0.37	1.68
1999	227	1.40	114.00	142.20	43.82	31.20	5.17	0.40	2.23

[a]Another estimation of the RUNJOB III chamber weight is given in [26,28] (260 kg).
[b]0.385 [29].
[c]2.28 [29].

tory is reconstructed by projecting each 3D coordinate on a plane of a 2D map. With reference to the map, the electron shower on nuclear emulsion plate can be detected with the use of a microscope. In order to identify the primary charge, one must find the interaction point (vertex point) and the primary track. All primary particles from the RUNJOB experiment were picked up by following back the shower (detected in the calorimeter) until its interaction point [5]. The identification of a gamma ray was made by observing "the feature of the cascade shower" [26]. According to RUNJOB, heavy primaries were identified "immediately without ambiguity" at nuclear emulsion plates above the vertex point, since "their tracks are of heavily ionizing ones associated with δ rays." Using background nuclei tracks as fiducials, the identification of helium and proton tracks was reportedly made with the location accuracy as "nearly the same" as JACEE [5]. RUNJOB reported that the track of proton primary can be missed in the long duration balloon flights due to "enormous background tracks" [30]. According to RUNJOB, in such difficult cases the "tracks near expected location" and the feature of secondary tracks and of cascade shower "were investigated very carefully" [30]. The percentage of the success ("some half among necessaries" [5]) in proton identification was reported only by RUNJOB [5]. The other half was assumed [5] "to be also protons (or 'neutrons produced via charge exchange in the atmosphere'), since helium and heavy primaries possibilities were rejected." RUNJOB explained that "practically we did not succeed in the perfect primary identification for all events, due to the presence of background tracks. Easily identified were the light elements (He, Li, Be) with grain densities higher than four times the minimum track density. Of course, unidentified events must be of proton (neutron), helium,..., or iron origin, and can not be anything else from a common-sense point of view. So, we assumed those unidentified events to be protons, since other elements (He, Li, ..., Fe) are identified definitely without ambiguity" [25].

C. Primary energy determination

It is necessary to convert the measured ΣE_γ into a spectrum in total energy. There is a large variance in the fraction of E_0 which is manifested as neutral pions. The dispersion is greater for protons and diminishes with increasing atomic mass. Because of the wide dispersion, E_0 cannot be determined from ΣE_γ for a single cosmic ray event. If the primary cosmic ray spectrum obeys a power law, then the ΣE_γ will be a power law as well [5,6]. The ΣE_γ spectrum follows a power law with the same index as the E_0 spectrum. Substitution of $\Sigma E_\gamma = C_{k\gamma}^{-1} E_0$ will reproduce the primary energy spectrum with the same normalization, where $C_{k\gamma}^{-1}$ is conversion factor. For the protons interacting in the RUNJOB target, the typical value $C_{k\gamma}^{-1}$ is ~ 0.27 [31], It was stated in [5] that the transition curves used for the determination of the electron shower energy were the same in the passive balloon-borne experiments JACEE and RUNJOB. Together with the photometric method of energy determination, RUNJOB also proposed and used several other methods [5,26,27].

D. Other corrections

It is usually pointed out that a balloon experiment utilizes a more complicated emulsion chamber than that for mountain experiments. Because of the technical complexities and limitations, estimation of the detection efficiency, as well as the conversion of observed energy to the primary energy, became a quite delicate procedure in each experimental case. The RUNJOB experiment has two objective obstacles—a large background [5] and not negligible effect of the atmospheric depth. The absolute intensity is obtained [5,32] using the relation $I = (\Sigma N \times e^{-\delta^2})/(\Sigma \xi S \Omega T e^{-t/\Lambda})$, where I is the absolute intensity, N is the observed number of primary, ξ is the detection efficiency, S is the geometrical chamber area, $\Omega$is the effective solid angle, $t$is the effective depth of observation, and $\Lambda$is attenuation length of the primary in the atmosphere. The factor $e^{-\delta^2}$ takes into account the fluctuation of the energy determination where $\delta = (\ln 10/\sqrt{2})\alpha\sigma$, α is the index of the integral power-law spectrum, and σ is the dispersion of the energy resolution. There were several reports on estimation [5,26,33] of the RUNJOB detection efficiency (with at least $\sim$10%–30% variations).

III. ANALYSIS AND RESULTS

A. Flight information

To be consistent in our analysis, we reexamined the flight data. For the purpose, we analyzed a variety of original sources of information [26–28]. The analysis is summarized in Appendix A. We conclude that incorrect evaluation of different data sets could happen at any stage and at any time of the experiment and analysis.

B. Simulation

In order to evaluate the experiment, we performed simulation calculations with input parameters listed in Table II. We assume a power-law primary spectrum in the form $dI/dE_0 = I_0 \times E_0^{-\beta}$, where I_0 is intensity, and β is the power-law index, at the top of atmosphere. Following the RUNJOB conclusion [5], we assumed [$I_0 = (2.26 \pm 0.13) \times 10^4$; $\beta = (2.78 \pm 0.05)$] for protons, and [$I_0 = (1.50 \pm 0.11) \times 10^3$; $\beta = (2.81 \pm 0.06)$] for helium nuclei. The intensity is given in units of $(\mathrm{m^2\,s\,str(GeV/n)})^{-1}$. The chamber area S, the exposure time T, the observational altitude t, and the effective solid angle Ω at the observational altitude t were either taken from [5,32] or estimated using the empirical fits to published data. To obtain the expected number of particles at

TABLE II. Numerical values used for simulation of events detected by the RUNJOB chamber. The proton attenuation length is 110 g/cm^2 [5,25,32]. The helium attenuation length is 48.67–49.68 g/cm^2 [5,25,32]. Square brackets show parameters used for the simulation set (PR-1). Parentheses show parameters used for the simulation set (PR-2), where the time duration of RUNJOB I is $T = 131$ h, and for RUNJOB II is $T = 168$ h. Input parameters for RUNJOB III and RUNJOB IV were the same for both simulation sets, (PR-1) and (PR-2).

Balloon	Effective altitude (g/cm^2) for proton	Effective solid angle for proton	Effective altitude (g/cm^2) for helium	Effective solid angle for helium	Exposure time (s)
RUNJOB I	(11.08[a])	(2.89[a])	10.94[a]	2.66[a]	469 800[a]
	[11.60[c]]	[$\sim$ 2.88[b]]	11.23[c]	$\sim$2.65[b]	[468 000[c]]
RUNJOB II	(10.64[a])	(2.90[a])	10.48[a]	2.67[a]	(604 800[a])
	[11.21[c]]	[$\sim$ 2.89[b]]	10.84[c]	$\sim$2.66[b]	[601 200[c]]
RUNJOB III	12.02[c]	$\sim$2.87[b]	11.60[c]	$\sim$2.65[b]	482 400[c]
RUNJOB IV	12.25[c]	$\sim$2.86[b]	11.85[c]	$\sim$2.64[b]	531 000[c]

[a][32].
[b]These estimations are based on [32]. We use the following empirical relations between the effective solid angle Ω and the effective altitude of observation t: for proton—$\Omega(t) = 3.141\,82 - 0.022\,73 \times t$; for helium—$\Omega(t) = 2.897\,83 - 0.021\,74 \times t$.
[c][5].

the observational altitude t, we have to take into account the attenuation factor $e^{-\tau}$, with $\tau = t/\Lambda$, where t is the observational altitude and Λ is the attenuation length of the primary in the atmosphere. To obtain the expected number of detected particles in the chamber in each energy bin, we have to use the detection efficiency ξ. We made the empirical fits to the graphic presentation of the detection efficiency ξ curves as a function of the primary energy E_0 (Fig. 6 from [5]) with parameters [34] listed in Table III. We performed simulations for primary proton and helium particles. One simulation set consists of 160 000 runs of RUNJOB 1995–1996 (exposition of eight chambers during ''578.5 h'' [5]) for each primary element. In the first proton simulation set of RUNJOB 1995–1996, we used the input parameters based on explicit numerical data [5] for the effective altitude, the exposure time, the chamber area, and the attenuation length. Using empirical fits to published data from [32] (see Table II), we estimated the effective solid angle. We call this simulated proton set (PR-1). In the second proton simulation set (PR-2) we assumed that the exposure time of RUNJOB I is $T = 131$ h, the exposure time of RUNJOB II is $T = 168$ h (see Appendix A). Another RUNJOB I, II parameters, such as the effective altitude, the effective solid angle, the chamber area, and the attenuation length were taken from [32] (see Table II). In this second proton simulation set (PR-2) the RUNJOB III, IV parameters were based on [5] and Table II [the same as the first simulation set (PR-1)]. For the helium simulation set of RUNJOB 1995–1996 (exposition of eight chambers during ''578.5 h'' [5]), we used the input parameters based on explicit numerical data [5] for the effective altitude, the exposure time, the chamber area, and the attenuation length. The empirical fit to published data from [32] (see Table II) was used for the estimation of the effective solid angle. All simulation sets used the detection efficiency $\xi(E_0)$ from Table III. In Appendix B we describe a detailed step-by-step simulation algorithm.

C. Experimental data

While paper [5] gives some glimpse on underlying statistics, the energy threshold value for the selection of the events in Table II (from [5]) was not reported explicitly. We did not find any publication which would mention fully and clearly defined numerical data based on full data [35]. The importance of the energy threshold can be seen from Fig. 1. This is an illustration of the observed number of

TABLE III. The fitting parameters estimated in the present work for the detection efficiency ξ reported by RUNJOB (see Fig. 6 from [5]). The fitting function is defined as $\xi(E_0) = B + (A - B)/(1 + e^{((E_0 - C)/D)})$ for protons in the 1995 chamber, and $\xi(E_0) = A + (B - A)/(1 + 10^{(C - E_0)*D})$ for helium in the 1995 chamber, as well as for protons and helium in the 1996 chamber, where A, B, C, and D are fitting parameters, and E_0 is a primary energy per nucleon. We have to note that the present fitting function for helium in the 1995 chamber is greater than zero in the energy region above $\sim E_0 = 3.19$. It means that below this value it is assumed that efficiency is close to zero. We noticed that similar critical value $\sim$3.180 is mentioned as one of the bin's boundaries in paper [25].

Primary particle	Year	A	B	C	D
Proton	1995	$-12.372\,87$	0.123	$-79.425\,23$	18.682 94
Helium	1995	$-14.902\,94$	0.229 23	$-35.496\,91$	0.046 86
Proton	1996	$-39\,086.6261$	0.165 99	$-76.417\,99$	0.067 81
Helium	1996	$-88.456\,15$	0.276 96	$-21.190\,45$	0.109 89

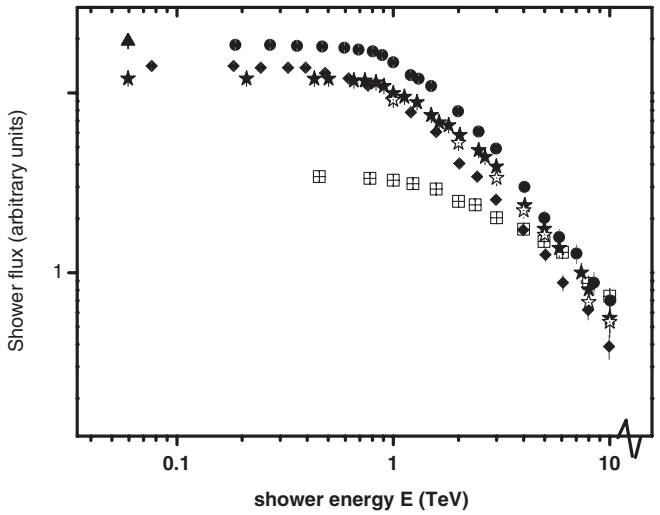

FIG. 1. Observation of showers detected in the RUNJOB calorimeter. Estimations are made on the basis of data from [26,28]. Squares with crosses: RUNJOB 1995 (20% of data). Rhombuses: RUNJOB 1996 (20% of data). Solid circles: RUNJOB 1997-5b (5% of data). Solid stars: RUNJOB 1999-10 (10% of data). Upward triangle: RUNJOB 1999-11 (10% of data). Open stars with dots show a simple average. Experimental points above 10 TeV were omitted due to insufficient clarity in the original image. The apparent difference between the observations can be explained by the detection conditions and the detection efficiency [5,25]. One can notice the effect of the detection threshold and detection efficiency in different observations [26]. The total number of detected showers was reported [26–28] as follows: RUNJOB I-II (four blocks)—381, RUNJOB III-IV (four blocks)—1497, RUNJOB VB (one block)—515, RUNJOB X (two blocks)—1193, RUNJOB XI (two blocks)—1131. The figure is for illustration purposes only.

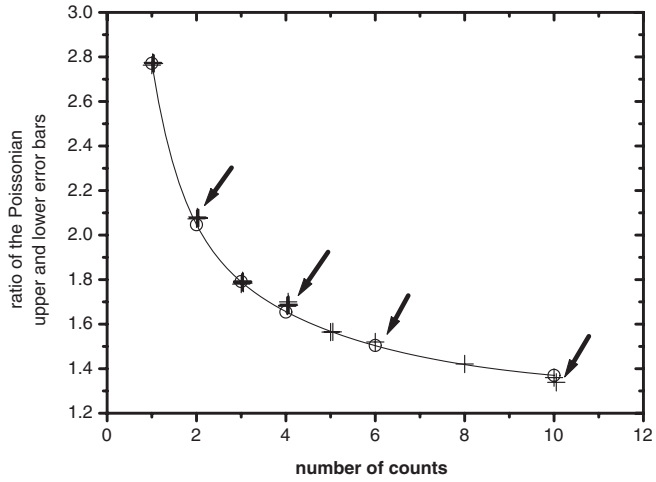

FIG. 2. Estimation of the actual observed counts on the basis of the ratio of the Poissonian upper and lower error bars reported by [36]. Based on Table I (from [36]), we calculate the ratio of the upper error bar (absolute value) to the lower error bar (absolute value). Open circles show theoretical points with the following coordinates on the x axis and the y axis: (1; 2.77), (2; 2.05), (3; 1.79), (4, 1.65), (6, 1.50), (10, 1.37). The line is drawn to guide the eye. Crosses show experimental data. There are 33 experimental points in this figure. These work estimations are based on [5,25]. Arrows indicate that there are some apparent deviations between the expected theoretical ratio for a given number of counts and the ratio calculated on the basis of the reported experimental data. We assume that the number of counts observed in experiment must be within the range 1–10 (since, only here, we can test the numerical data from [36]), taking a nearest integer number in these estimations. Our choices are shown in the figure as well as in Tables IV, V, VI, VII, VIII, and IX. We use here some slight variations (± 0.05) in the x-axis coordinates of points for illustration purposes only.

showers in different experiments based on figures from [26,28]. An obvious difference between the observations was explained by the detection conditions and the detection efficiency [26,28]. The raw number of events, in particular energy bins, can be estimated from the reported numerical energy spectra. Comparison of the tabulated energy spectra (Table 4 from [5]) with the figures from [5] shows that there is an incorrect caption in Table 4 from [5]: instead of energy ''per particle'' there must be energy ''per nucleon.'' Experimental points show $J \pm \Delta_J$, where the reported errors Δ_J are statistical [5,26]. If $\Delta_{J_+} = \Delta_{J_-}$, then $N \sim 1/\delta^2$, where $\delta = \Delta_J/J$, and N is the raw number of particles. Since ''the statistics of high energy events is small in general in the cosmic ray experiments,'' the error bars in the RUNJOB report were ''evaluated on the basis of the Poissonian distribution,'' not the Gaussian one [see [36] mentioned in [5]]. As one can see in [5,25], in such cases $\Delta_{J_+} \neq \Delta_{J_-}$, and one must use some special technique to go back to the original number of counts N. We show in Fig. 2 that, using the ratio of the upper and the lower limits of the errors Δ_{J_+} and Δ_{J_-}, it is possible to estimate the raw number of events in each bin. Figure 2 can be useful for a quick evaluation of the number of counts in the case when only the picture (and not the explicit numerical data) is available. Of course, the accuracy in the evaluation of the number of counts in that case would be lower (and can deviate from the expected ratio) than the one based on the explicit numerical data. We noticed that there are several discrepancies between the expected ratio for a given number of counts [36] and the experimental ratio (indicated by arrows in Fig. 2). Generally, we assume that the number of counts obtained in simulation can be a ''real'' number, but a number of counts observed in the present experiment must be an ''integer'' number. Here (Fig. 2) the situation is slightly different. During our reanalysis, we found another explicit numerical data of the same RUNJOB 1995–1996 exposition [5], based on a different version of the chamber efficiency correction [25]. Tables IV and V show our estimations of the raw number of primary tracks based on data from RUNJOB 1995–1996 [5] and the average number of simulated events in each energy bin. Tables VI, VII, VIII, IX, and X show other estimations of the raw number of events deduced from the RUNJOB reports

TABLE IV. Fluxes and raw number of protons from RUNJOB 1995–1996 flights reported by [5]. Flux is given in units of $(m^2\ s\ str(GeV/n))^{-1}$. Mark "sum" stands for the summation of the RUNJOB 1995 and RUNJOB 1996 counts. Mark "TeV/n" stands for "energy per nucleon." Mark "sd" stands for standard deviation. The simulated numbers were rounded up to three decimal places. The RUNJOB 1996 simulation is based on Table II and [5]. See footnotes for the RUNJOB 1995 simulation.

Bin	Energy TeV	Flux[a]	Detected N_{exp}	Expected $\langle N_{sum}\rangle \pm$ sd	Expected $\langle N_{1995}\rangle \pm$ sd	Expected $\langle N_{1996}\rangle \pm$ sd
	TeV		Estimation[a]	Simulation	Simulation	Simulation
1	8–14	$1.46^{+0.25}_{-0.25}(-7)$	34	$(138.146 \pm 39.262)^b$ $(138.484 \pm 39.300)^c$	$(23.155 \pm 9.097)^b$ $(23.493 \pm 9.262)^c$	(114.991 ± 38.244)
2	14–26	$2.80^{+0.57}_{-0.57}(-8)$	24	$(85.849 \pm 23.998)^b$ $(86.252 \pm 24.098)^c$	$(24.970 \pm 10.540)^b$ $(25.373 \pm 10.765)^c$	(60.879 ± 21.593)
3	26–42	$5.77^{+1.02}_{-1.02}(-9)$	32	$(31.259 \pm 9.156)^b$ $(31.451 \pm 9.128)^c$	$(11.858 \pm 5.478)^b$ $(12.051 \pm 5.430)^c$	(19.400 ± 7.351)
4	42–70	$1.56^{+0.38}_{-0.38}(-9)$	17	$(15.340 \pm 4.891)^b$ $(15.415 \pm 4.951)^c$	$(6.571 \pm 3.283)^b$ $(6.646 \pm 3.371)^c$	(8.769 ± 3.634)
5	70–140	$2.95^{+1.35}_{-0.95}(-10)$	8	$(7.768 \pm 2.760)^b$ $(7.830 \pm 2.752)^c$	$(3.508 \pm 1.900)^b$ $(3.571 \pm 1.888)^c$	(4.259 ± 2.007)
6	140–500	$1.84^{+1.78}_{-1.00}(-11)$	3	$(2.928 \pm 1.262)^b$ $(2.945 \pm 1.297)^c$	$(1.331 \pm 0.855)^b$ $(1.349 \pm 0.906)^c$	(1.596 ± 0.930)
7	500–3000	$8.80^{+20.2}_{-7.31}(-13)$	1	$(0.012 \pm 0.045)^b$ $(0.012 \pm 0.045)^c$	$(0.004 \pm 0.019)^b$ $(0.003 \pm 0.019)^c$	(0.008 ± 0.040)
			Total: 119	$Total_{sum}$: $(281.301 \pm 78.862)^b$ $(282.388 \pm 79.047)^c$	$Total_{1995}$: $(71.398 \pm 30.669)^b$ $(72.485 \pm 31.141)^c$	$Total_{1996}$: (209.903 ± 72.761)

[a]Based on energy spectra and flux from [5]. See also Table II.
[b]This is simulation set (PR-1). The flight duration of RUNJOB I is assumed to be 130 h, and RUNJOB II is assumed to be 167 h. Other RUNJOB I, II parameters are based on numerical data from [5] and Table II.
[c]This is simulation set (PR-2). The flight duration of RUNJOB I is assumed to be 131 h, and RUNJOB II is assumed to be 168 h. Other RUNJOB I, II parameters are based on numerical data from [32] and Table II.

[5,25]. Figures 3–7 illustrate experimental energy spectra of elements from different expositions.

D. Data evaluation

Let us compare the results of our simulation with the reported experimental observation (see Tables IV and V for proton and helium). We can notice three distinctive groups in the energy region 8–3000 TeV for protons: (1) in the first two bins (8–26 TeV) the number of counts in experiment is much lower than that in simulation; (2) in bins 3–6 (26–500 TeV) the number of counts in experiment is very close to the expected mean values (averaged over the 160 000 runs, see Appendix B) in simulation; (3) experiment and

TABLE V. Fluxes and raw number of helium nuclei from RUNJOB 1995–1996 flights reported by [5]. Marks and units are the same as in Table IV.

Bin	Energy TeV	Flux[a]	Detected N_{exp} This work	Expected $\langle N_{sum}\rangle \pm$ sd This work	Expected $\langle N_{1995}\rangle \pm$ sd This work	Expected $\langle N_{1996}\rangle \pm$ sd This work
			Estimation[a]	Simulation[a]	Simulation[a]	Simulation[a]
1	2.5–6.25	$1.13^{+0.29}_{-0.29}(-7)$	15	(53.484 ± 19.626)	(6.553 ± 2.554)	(46.931 ± 19.484)
2	6.25–9.5	$1.98^{+0.83}_{-0.62}(-8)$	10[b]	(17.363 ± 5.980)	(5.312 ± 2.233)	(12.051 ± 5.555)
3	9.5–17	$4.04^{+1.70}_{-1.25}(-9)$	10[b]	(13.586 ± 4.831)	(5.121 ± 2.360)	(8.465 ± 4.222)
4	17–25	$1.06^{+0.85}_{-0.50}(-9)$	4[c]	(4.483 ± 1.811)	(2.014 ± 1.133)	(2.468 ± 1.416)
5	25–75	$1.45^{+1.16}_{-0.69}(-10)$	4[c]	(4.207 ± 1.850)	(1.980 ± 1.211)	(2.227 ± 1.402)
			Total: 43	$Total_{sum}$: (93.123 ± 32.305)	$Total_{1995}$: (20.981 ± 8.901)	$Total_{1996}$: (72.142 ± 31.097)

[a]Based on energy spectra and flux from [5]. See also Table II.
[b]We assume that the number of counts here is an integer number $N = 10$. See also Fig. 2.
[c]We assume that the number of counts here is an integer number $N = 4$. See also Fig. 2.

TABLE VI. Fluxes and raw number of protons and helium nuclei from RUNJOB 1995–1996 flights reported by [25]. Marks and units are the same as in Table IV.

Energy TeV	Flux[a] Protons	N This work	Energy TeV	Flux[a] Helium	N This work
10–14	$1.194^{+0.281}_{-0.281}(-7)$	18	1.383–3.180	$6.197^{+1.005}_{-1.005}(-7)$	38
14–22	$3.748^{+0.765}_{-0.765}(-8)$	24	3.180–4.148	$1.678^{+0.433}_{-0.433}(-7)$	15
22–36	$9.025^{+2.189}_{-2.189}(-9)$	17	4.148–5.530	$5.425^{+1.716}_{-1.716}(-8)$	10
36–60	$2.424^{+0.485}_{-0.485}(-9)$	25	5.530–8.986	$1.740^{+0.435}_{-0.435}(-8)$	16
60–140	$3.978^{+1.027}_{-1.027}(-10)$	15	8.990–22.12	$'2.641^{+0.660}_{-0.660}(-9)$	16
140–500	$1.696^{+1.639}_{-0.916}(-11)$	3	22.12–69.13	$1.596^{+1.277}_{-0.758}(-10)$	4
500–2000	$1.336^{+3.073}_{-1.109}(-12)$	1			
		Total: 103			Total: 99

[a]Based on energy spectra from [25].

simulation are different in the last bin (500–3000 TeV). In the case of helium events in the energy region 2.5–75 TeV/n (5 bins), we can notice a large difference between simulation and experiment in the first bin (2.6–6.25 TeV).

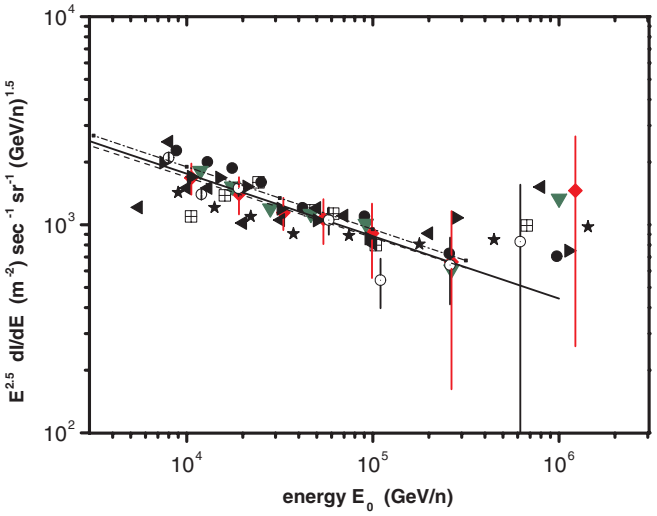

FIG. 3 (color online). Proton energy spectra. Compilation of the reported measurements from the RUNJOB observations: (20% of data—exposition 1995 [26] (squares with crosses); 35%—1995–1996 [26] (leftward triangles); 40%—1995–1996 [25] (downward triangles); 40%—1995–1996 [5] (rhombuses); 45%—1995–1997 [26] (solid circles); all the data with sum of gamma ray energies greater than 5 TeV—1995–1999 [37,38,50,51] (rightward triangles); full data—1995–1999 [4] (stars). The JACEE [9] data are presented for comparison. Solid line: proton spectrum with power index $\beta = 1.8$. The dashed line shows the best fit to the data set from [5], and the dash-dotted line—to the data set from [25]. These best fits are shown in numerical form in Table XI (estimations without errors dE in energy variables). For clarity most of the error bars were omitted.

1. Quantitative evaluation

Let us consider two choices: the null hypothesis and the alternative hypothesis. The null hypothesis here is that the reported experimental observation is obtained by chance. The alternative hypothesis is that the reported experimental observation was affected by something else. Thus, at the end of the analysis we can hope to know only the odds that the null hypothesis is true. For this purpose we can use the χ^2 test with $\chi^2 = \sum(N_{\rm obs} - N_{\rm sim})^2/N_{\rm sim}$, where $N_{\rm obs}$ is the experimental number of counts deduced (this work) from the reported flux, and $N_{\rm sim}$ is the expected number of occurrences from our simulation (see Tables IV and V). The expected value here is assumed to be the mean value (averaged over the entire counts) in the bin. In Fig. 8 we show a comparison of the obtained χ^2 values with the theoretical critical χ^2 values for different significance levels of α [39]. To avoid systematic shift to high χ^2 values in

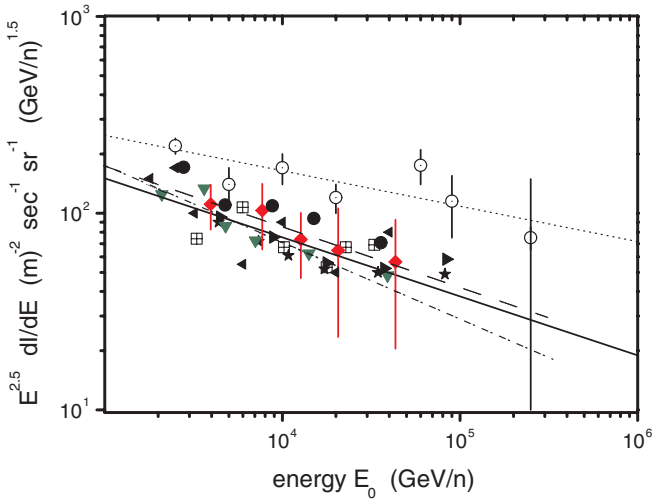

FIG. 4 (color online). Helium energy spectra. Compilation of the reported measurements from the RUNJOB observations. Solid line: $\beta = 1.8$. Dotted line: $\beta = 1.68$. Marks are the same as in Fig. 3.

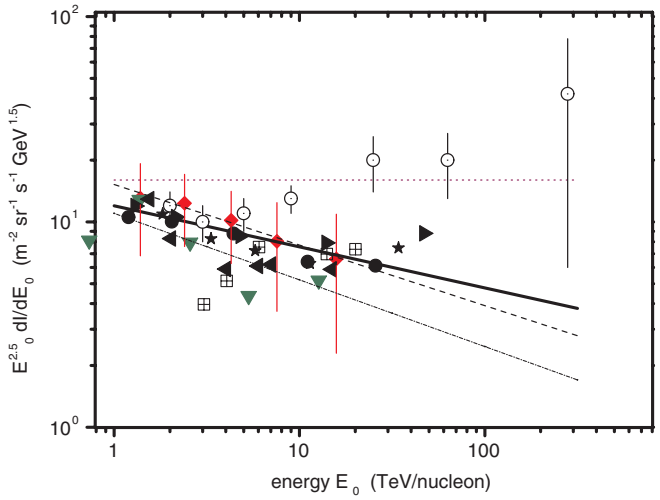

FIG. 5 (color online). CNO energy spectra. Compilation of the reported measurements from the RUNJOB observations. Marks are the same as in Fig. 3. Solid line: $\beta = 1.7$. Dotted line: $\beta = 1.5$.

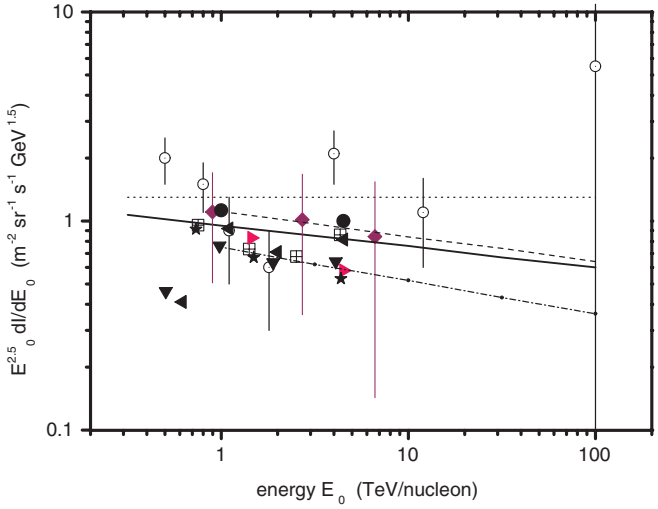

FIG. 7 (color online). Iron energy spectra. Compilation of the reported measurements from the RUNJOB observations. Marks are the same as in Fig. 3. Solid line: $\beta = 1.6$. Dotted line: $\beta = 1.5$.

this figure, the bin 500–3000 TeV for protons (the 7th bin from Table IV) was not included. Thus, only six bins in the energy interval 8–500 TeV for protons were taken into account in Fig. 8. It is possible to consider several choices of possible independent sets of the experimental bins (6, 5, 4, 3, 2) for protons and (5, 4, 3, 2) for helium. The number of degrees of freedom is defined here as $df = N_{\mathrm{bin}} - 1$, where N_{bin} is the number of bins. Figure 8 shows correlation between chi-square values and the number of degrees of freedom for different significance levels of protons (crosses and triangles) and helium (squares). Crosses show chi-square values based on (PR-1) simulation set, triangles—on (PR-2) set. The thick line with two arrows illustrates the 95%–5% region of significance levels α. Usually, if the χ^2 value is above the chosen critical value (for instance, $\alpha = 5\%$), then we must reject the null hypothesis at $\alpha = 5\%$ level. However, sometimes it is interesting to know the probability of the outcomes with χ^2

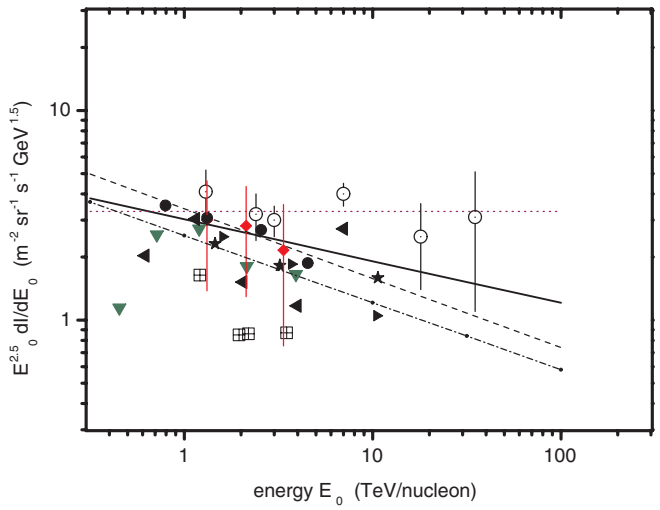

FIG. 6 (color online). NeMgSi energy spectra. Compilation of the reported measurements from the RUNJOB observations. Marks are the same as in Fig. 3. Solid line: $\beta = 1.7$. Dotted line: $\beta = 1.5$.

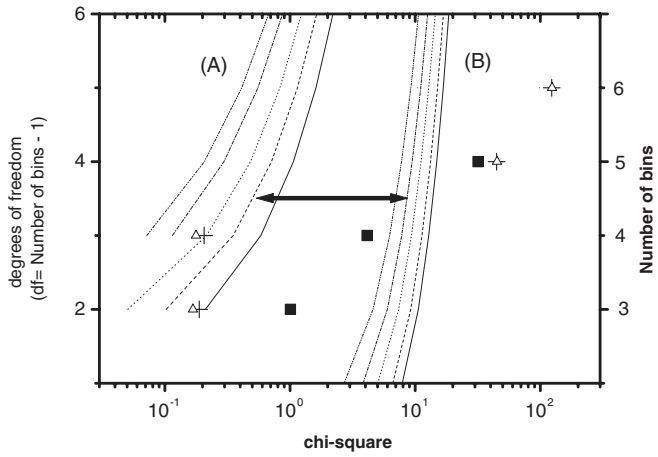

FIG. 8. Correlation between χ^2 values and the number of degrees of freedom for different significance levels α. Crosses and triangles stand for proton events [simulation sets (PR-1) and (PR-2)], and squares—for helium events. Crosses and squares show the result of the simulation set (PR-1) (see Table II and [5]). Open triangles show the result of simulation (PR-2) with an assumption that the flight duration of RUNJOB I is $T = 131$ h, and RUNJOB II—168 h, with the effective altitudes for these flights from [32] and other parameters from Table II and [32]. The thick line with arrows at both ends shows $\alpha = 0.95$–0.05 area. The "A" set: $\alpha = 0.900$ (solid line); $\alpha = 0.950$ (dash line); $\alpha = 0.975$ (dotted line); $\alpha = 0.990$ (dash-dotted line); $\alpha = 0.995$ (dash-dot-dotted line). The "B" set: $\alpha = 0.005$ (solid line); $\alpha = 0.010$ (dashed line); $\alpha = 0.025$ (dotted line); $\alpha = 0.050$ (dash-dotted line); $\alpha = 0.100$ (dash-dot-dotted line).

values less than the critical value $\alpha = 95\%$. These are so-called ''too good'' measurement cases. In our Fig. 8 this would be an area to the left from the $\alpha = 95\%$ line (dash line). We can see that the calculated χ^2 values are sensitive to the input parameters such as the exposure time and the effective depth of the observation [see triangles in Fig. 8 for the (PR-2) simulation]. The χ^2 point (cross point at $df = 4$) stays outside the allowed critical value of $\alpha = 95\%$, and even beyond $\alpha = 97.5\%$. This would mean the rejection of the null hypothesis for four bins in the energy region 26–500 TeV, since there is very low probability to obtain this ''precise'' result by chance. As for the case of seven bins for protons (crosses and triangles) and five bins for helium (squares), the χ^2 values that we calculated are larger than those predicted by theory even for $\alpha = 0.005\%$.

2. What does this experimental observation mean?

We can define the reported experimental observation as follows: exposition of eight chambers during ''578.5 h'' [5] with detection of protons in the energy region 8–3000 TeV (seven bins) and helium particles in the energy region 2.5–75 TeV/n (five bins). We can conclude that there is close to zero chance that the reported experimental observation and simulation are different by chance. The null hypothesis here can be rejected. Thus, the reported experimental observation was affected by something else. For instance, we can consider the following interpretations.

(1) If the reported experimental observation was based on the explicit trigger conditions stated by paper (eight chambers during 578.5 h were used to obtain ''these spectra''), then the observed counts in the first two bins (the energy region 8–26 TeV) for protons would be consistent with an assumption of a much lower proton flux. If so, it is not surprising that the reported [5] RUNJOB helium flux in the energy region ~8–26 TeV/n is systematically lower than that of JACEE. In the energy region 26–500 TeV/n there were only four helium events, and the low intensity is consistent with very small experimental statistics. One can see that the intensities of heavy nuclei reported by RUNJOB are also systematically lower than that reported by JACEE (see Figs. 5–7 and Tables VII, VIII, and IX).

(2) Using Tables V and VI, one can notice that apparently there could be some selection of experimental events for the helium spectra. Namely, one can notice 43 events in the energy region 2.5–75 TeV/n in Table V against 61 events in the energy interval 3.18–69.13 TeV from Table VI. The conversion factors C_γ for helium events were within ~5% there. We did not find an explicit description of a specific procedure which would systematically explain these counts [5,25]. In general, if there was some methodical procedure applied to the selection of individual experimental events, and this procedure was not explicitly described or presented in a quantitative form, then it would be quite reasonable to assume the existence of bias in the reported experimental observation.

(3) We have to mention also the specific experimental setting here. The identification of proton and helium events was reportedly made in the conditions of heavy background tracks in the whole energy interval of our concern. This fact alone could explain, in principle, an apparent low number of the reported events at low energies (see Tables IV and V). We can note that all the long duration balloon flights performed at similar altitudes (RUNJOB, MUBEE) mentioned high density of background tracks, which significantly hamper the efforts to identify showers correctly (protons and helium tracks). At the same time the similar passive chamber from the Sanriku experiment [40,41], which had flown for a short period of time (for ~30 h) at the low altitude (~ 32.8 g/cm^2), did not suffer from significant background noise [40], and reported the flux of protons and helium nuclei similar to that of JACEE in the energy region ~3–10 TeV/n. We

TABLE VII. Fluxes and raw number of CNO nuclei. Marks and units are the same as in Table IV.

Energy TeV	Flux[a]	N This work	Energy TeV	Flux[b]	N This work
1.07–1.79	$1.83^{+1.47}_{-0.87}(-8)$	4	0.519–1.037	$5.575^{+3.026}_{-1.991}(-7)$	6
1.79–3.21	$4.38^{+2.63}_{-1.68}(-9)$	5	1.037–1.815	$1.840^{+0.531}_{-0.531}(-7)$	12
3.21–5.71	$8.49^{+5.10}_{-3.26}(-9)$	5	1.815–3.630	$2.378^{+0.717}_{-0.717}(-8)$	11
5.7–10.0	$1.62^{+1.57}_{-0.88}(-10)$	3	3.630–7.779	$2.119^{+1.695}_{-1.007}(-9)$	4
10.–25.	$2.10^{+2.84}_{-1.37}(-11)$	2	7.78–20.74	$2.854^{+3.853}_{-1.855}(-10)$	2
		Total: 19			Total: 35

[a]Based on energy spectra from [5].
[b]Based on energy spectra from [25].

TABLE VIII. Fluxes and raw number of NeMgSi nuclei. Marks and units are the same as in Table IV.

Energy TeV	Flux[a]	N This work	Energy TeV	Flux[b]	N This work
			0.3571–0.5713	$2.643^{+6.078}_{-2.194}(-7)$	1
			0.5713–0.8927	$1.878^{+1.815}_{-1.014}(-7)$	3
1.04–1.67	$4.76^{+4.60}_{-2.57}(-8)$	3	0.893–1.607	$5.497^{+4.398}_{-2.611}(-8)$	4
1.67–2.71	$1.35^{+1.31}_{-0.73}(-8)$	3	1.607–2.857	$8.505^{+8.222}_{-4.593}(-9)$	3
2.71–4.17	$3.29^{+4.44}_{-2.14}(-9)$	2	2.857–5.356	$1.730^{+2.336}_{-1.125}(-9)$	2
		Total: 8			Total: 13

[a]Based on energy spectra from [5].
[b]Based on energy spectra from [25].

can also recall that the Grigorov experiment in space showed lower flux not only for helium but for protons as well [40,42,43]. Thus, the discrepancy with JACEE would be consistent with an assumption that the systematics between different techniques was involved. We should not forget that the subjective factor in the evaluation of a particular shower is not negligible, especially in the case of passive emulsion chamber experiments [17,18]. It is important to remember that interpretation of a signal recorded in emulsions is primarily based on visual evaluation. It is well known that, when one is looking at a fixed object (for instance, a dark spot on a film) in a complex physical environment (especially with heavy background), then it is much harder to divert one's primary attention to some new object. Thus, while searching for an object in a successive layer, one might have specific foretaste regarding the anticipated object, thus slightly evaluating expectation ahead of the reality outcome.

E. PeV event

The RUNJOB experiment reported an observation of "a single proton" with primary energy around 10^{15} eV as an indication of "the absence of a cut-off region somewhere around 100 TeV" [5]. Taking into account that the observational altitude in the experiment was 10–12 g/cm^2, and the arrival zenith angle of this particle was determined as $\theta \sim 64.5$ degrees, the slant depth would be around $\sim$30 g/cm^2. In our simulation we confirmed that this is a very rare event with a small probability of happening, in particular, an experiment with limited exposition (see Table IV). Yet, given enough repetitions of the situation over a long period of time (about 1 order of magnitude higher in exposition, than that of RUNJOB 1995–1996), the event is bound to happen. This just occurred by chance, eventually after a long string of many experiments. In fact, the particle itself could be not a primary proton, but a spectator nucleon from an interaction of a heavy primary particle with an air nucleus. Considering an individual shower, it is impossible to determine whether it is originated by a primary proton or by a nucleon from a heavy primary nucleus. It could indicate the arrival of a cosmic ray family produced by a heavy primary nucleus [22,44]. In general (not only for 1 PeV event), if secondary nucleons from heavy primaries were accounted as protons, some heavy primaries would be missing. It is not unusual that some families could be detected, but not recognized. The

TABLE IX. Fluxes and raw number of Fe nuclei. Marks and units are the same as in Table IV.

Energy TeV	Flux[a]	N This work	Energy TeV	Flux[b]	N This work
0.45–1.79	$4.58^{+4.43}_{-2.48}(-8)$	3	0.3571–0.7143	$8.042^{+18.5}_{-6.675}(-8)$	1
1.79–4.11	$2.65^{+3.58}_{-1.72}(-9)$	2	0.714–1.339	$2.548^{+2.463}_{-1.376}(-8)$	3
4.1–10.7	$2.36^{+5.44}_{-1.96}(-10)$	1	1.339–2.679	$4.061^{+5.483}_{-2.640}(-9)$	2
			2.679–6.250	$5.975^{+13.74}_{-4.959}(-10)$	1
		Total: 6			Total: 7[c]

[a]Based on energy spectra from [5].
[b]Based on energy spectra from [25].
[c]Our estimation of spectra from [37,38] indicated that there were still seven iron nuclei in the sample of "all data" with shower energy "above 5 TeV."

TABLE X. Statistics of cosmic ray primaries reported by RUNJOB [5,25,26]. Estimation of the number of primary tracks in the energy spectra of cosmic ray primaries reported by RUNJOB [5,25,26]. Experimental points show $J \pm \Delta_J$. For statistical errors, if $\Delta_{J_+} = \Delta_{J_-}$, then $N \sim 1/\delta^2$, where $\delta = \Delta_J/J$. If $\Delta_{J_+} \neq \Delta_{J_-}$, then see Ref. 47 in [5] for details. The fraction of the events included in spectra (our estimation) is much lower than the total observed number of primary tracks. One has to remember that there is a misprint in Table IV [5]. Instead of GeV/particle there should be GeV/nucleon. NA stands for "not available."

Set	Source	Comment	Year	Proton	He	LiBeB	CNO	NeMgSi	Sub-Fe	Fe	All ($p, \ldots,$ Fe)
1	[5]	Four blocks	1995	117	26	3	9	6	3	6	170
2	[26]	Three blocks	1996	355	83	12	30	9	4	2	495
3	[5]	Four blocks	1996	339	90	12	33	11	4	2	491
4	[5,25]	set(1) + set(3)	1995–1996	456	116	15	42	17	7	8	661
5[a]	[25]	This work	1995–1996	103	99	NA	35	13	NA	7	257
6[b]	[5]	This work	1995–1996	119	43	NA	19	8	NA	6	195

[a]Based on energy spectra from [25].
[b]Based on energy spectra from [5].

result depends on applied methods. Spectator nucleons or leading nucleon can easily mimic primary protons [18].

F. The energy spectra of cosmic ray primaries

The purpose of this section is to analyze the experimental spectra indices reported by RUNJOB. We found above that there was practically zero probability to obtain the reported number of events in seven bins of protons and five bins of helium based on eight chambers from 578.5 h exposition [5]. Nevertheless, to be consistent in our study, we use here the explicit numerical data on primary fluxes reported by [5,25]. The energy spectra consist of binned data of flux versus energy [5,25]. RUNJOB reportedly used "the method of least squares" for fitting "a power-like spectrum" onto their data [5].

1. Estimation of the spectra indices

Since we did not know the exact fitting program used by RUNJOB, we have searched for a procedure which would report errors of the fitted slopes as small (~ 0.05–0.06) as the ones reported by RUNJOB for proton and helium [5]. To be objective, we choose an independent fitting procedure from [45]. As a test, we applied this procedure to the tabulated numerical data from [46], and found that the result of the fitting [45] ($\beta \pm \Delta\beta = -2.73 \pm 0.06$) agreed with the index of the power-law function reported by [46] (-2.73 ± 0.06). Then, on the basis of the numerical data on flux presented in our Tables IV, V, VI, VII, VIII, and IX (based on [5,25]), and using the fitting procedure from [45], we estimated the indices of the best fit power-law functions for RUNJOB. To do this, for each given energy bin (E_1; E_2) we calculate the geometrically weighted energy $\langle E\rangle = \sqrt{E_1 * E_2}$ (the abscissa). The flux (the ordinate) values were taken from Tables IV, V, VI, VII, VIII, and IX (based on [5,25]). If the upper and the lower error bars were different, we use a simple average value as an error estimate. Using available options from [45], we could consider two fitting choices: either use errors (dE) for each energy bin estimate $\langle E\rangle$, or not use (as in the case of our test for [46]). In our choice of the error (dE), we assumed that both numerical values, ($\langle E\rangle + dE$) and ($\langle E\rangle - dE$), should be contained within the energy bin (E_1; E_2) (some slight variations in the magnitude of dE appeared to be not crucial here). To estimate indices of the power-law spectra, we also applied an original method from [19,47]. We call this method as "g-method" hereafter. According to the g-method, if flux follows power law $J(E) \sim E^{-\beta}$, then the power index $\langle\beta\rangle = \Sigma(\beta_i/\sigma_i^2)/\Sigma(1/\sigma_i^2)$, and $\sigma_i = \sqrt{(1/(N_i + 1/N_{i+1}))}/\ln(E_i/E_{i+1})$, since $\sigma(J_i)/J_i = 1/\sqrt{N}$, where i stays for a bin number, and N_i is a number of counts in the bin i. Table XI presents our estimations. For each primary particle we present three estimations of the power-law indices: (1) based on [45] without errors (dE) in energy, but with errors in flux; (2) based on [45] with errors (dE) in energy, as well as in flux; (3) based on g-method. The estimations by the first method [45] are presented in Table XI in the following format: (power index and the error of the power index; the number of data points used for the estimation; the reduced chi-square value). According to the definition, the reduced chi square is the χ^2 value divided by the number of degrees of freedom. The power-index errors [45] show the level of fluctuations seen in the data. Numerical values obtained by the g-method are shown in square brackets in Table XI.

2. Evaluation of the energy spectra

(1) We can conclude that the errors ($\Delta\beta \sim 0.05$–0.06) of the power indices of proton and helium spectra reported by RUNJOB [5] are not statistical. For instance, in case of helium, if the error $\Delta\beta \sim 0.06$ were statistical, one would have expected $1/(0.06/2.81) \sim 2193$ detected particles. Certainly this is not the case here (see Tables VI and X). The RUNJOB errors of power indices show the degree of deviation of experimental data points from a straight line. Most likely, the reported RUNJOB errors of the power indices reflect the result of the data evaluation by the applied fitting program.

TABLE XI. Indices of the best fit power-law function. Estimations are based on Tables IV, V, VI, VII, VIII, and IX. Original data are from [5,25]. "N" stands for "number of primary particles." "R.c.s" stands for "reduced chi square." The estimations by the method from [45] are presented in the following format: (power index and the error of the power index; the number of data points used for the estimation; R.c.s). The first line in parentheses shows estimations using errors in flux values for each bin, but without use of errors in energy (dE). The second line in parentheses shows estimations using errors in energy (dE) and errors in flux values for each bin. Numerical values obtained by the g-method are shown in square brackets. See the text for additional explanations.

Primary	Index,[a] Number of bins, R.c.s This work Estimate	N[a] This work Estimate	Index,[b] Number of bins, R.c.s This work Estimate	N[b] This work Estimate	Index[c] 40% data RUNJOB	Index[c] Full data RUNJOB
p	(2.79 ± 0.02; 6; 0.028) (2.78 ± 0.02; 6; 0.005) [2.79 ± 0.25]	119	(2.80 ± 0.03; 6; 0.094) (2.82 ± 0.04; 6; 0.021) [2.81 ± 0.27]	103	2.78 ± 0.05	2.74 ± 0.08 2.78 ± 0.06[d]
He	(2.81 ± 0.05; 5; 0.050) (2.85 ± 0.07; 5; 0.023) [2.77 ± 0.42]	43	(2.89 ± 0.14; 6; 0.27) (2.97 ± 0.14; 6; 0.12) [2.70 ± 0.29]	99	2.81 ± 0.06	2.78 ± 0.20 2.74 ± 0.12[d]
CNO	(2.80 ± 0.04; 5; 0.010) (2.83 ± 0.04; 5; 0.004) [2.78 ± 0.60]	19	(2.82 ± 0.28; 5; 0.79) (2.84 ± 0.19; 5; 0.25) [2.76 ± 0.40]	35	~2.7	~2.7
NeMgSi	(2.83 ± 0.14; 3; 0.012) (2.85 ± 0.15; 3; 0.010) [2.82 ± 0.83]	8	(2.82 ± 0.13; 4; 0.039) (2.81 ± 0.12; 4; 0.027) [2.78 ± 0.82][e]	13		
Fe	(2.62 ± 0.04; 3; 0.002) (2.63 ± 0.04; 3; 0.002) [2.61 ± 0.71]	6	(2.66 ± 0.10; 3; 0.007) (2.65 ± 0.09; 3; 0.006) [2.65 ± 1.04][f]	7	~2.55	~2.6

[a][5].
[b][25].
[c][4].
[d][48].
[e]Based on four data points (12 events).
[f]Based on three data points (six events).

(2) Considering our estimations presented in Table XI, we can see that in most of the cases, for all primaries, the reduced chi-square values are very small (far from unity). In other words, the experimental data show much smaller fluctuations from the fitted curve than the expected one for a given statistics [45]. This behavior of a signal is consistent with an assumption that the measurement errors were systematic rather than random [45]. Systematic errors are usually the result of biases introduced by applied methods. Generally it is believed that, if the experimental sample size increases, then the effect of random error would tend to decrease. For instance, one can notice that the experimental helium and CNO spectra (see Table XI) show rather peculiar behavior. Let us compare the errors for power indices based on [5] ($\Delta\beta = 0.05$–0.07 for helium, $\Delta\beta = 0.04$ for CNO) and [25] ($\Delta\beta = 0.14$ for helium and $\Delta\beta = 0.28$–0.19 for CNO) with the corresponding statistics ($N = 43$ [5] and $N = 99$ [25] for helium and $N = 19$ [5] and $N = 35$ [25] for CNO). As we can see, the tendency here is just opposite to the general expectation.

(3) The error bars of the power indices estimated by the g-method reflect the square root of the number of events in the experimental bin, they are statistical errors. One can see that the statistical errors are large due to the small number of events. It is obvious that the reported indices for different primaries would agree within the large error bars. Thus, there is no solid basis to discuss some regularities (finer than the accuracy of the method) between the behavior of specific power spectra indices of different elements.

(4) We can conclude that, given the large methodical and statistical uncertainties in the RUNJOB spectra indices, one cannot choose one particular version of the primary composition from a variety of possibilities in the concerned energy region.

G. Primary mass

Mean values of the logarithm of mass number can be considered as the indicator of the composition [5,25]. It is expressed as $\langle \ln A \rangle(E_p) = \Sigma \Delta J_m(\ln A_m)/\Sigma \Delta J_m$, where ΔJ_m is a differential intensity for the element m with

mass number A_m in the energy bin $(E_p, E_{p+\delta p})$. In Fig. 9 we show mean values of the logarithm of mass number A (the average mass $\langle \ln A \rangle$) reported by RUNJOB, together with our estimations based on Table XI (estimations without errors dE in energy variables). We assume that the power index does not change with energy for each primary component in the limited energy interval of our concern. For instance, one can see that, if the spectra behaved as reported by RUNJOB [4,5], then the average mass would increase (see the solid line in Fig. 9). In other words, the statement that "the RUNJOB data show a constant average mass up to 1 PeV/particle" [4] contradicts here to the behavior of individual energy spectra concluded by RUNJOB. The primary mass would increase even if one uses the best fit to the RUNJOB data *itself* (using the mean values of primary spectra indices with estimations without errors dE in energy variables), without any reference to the "other" uncalibrated experiments (see dashed line and dash-dotted line in Fig. 9).

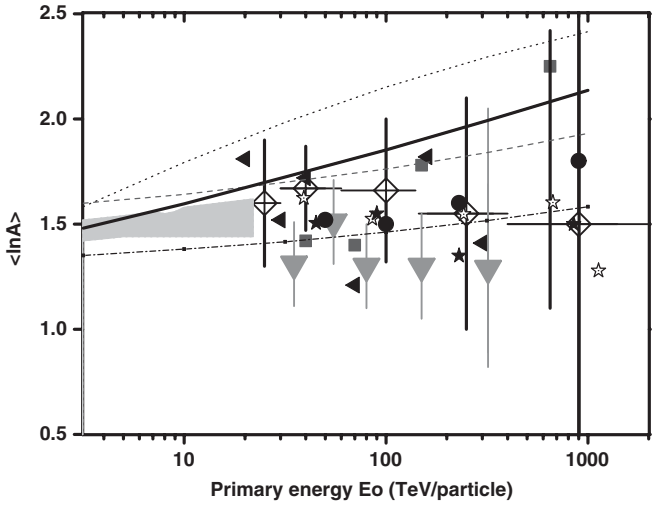

FIG. 9. Comparison of the average mass $\langle \ln A \rangle$ evaluated by RUNJOB in different observations. Squares with crosses: 20% of data—1995 exposition [26,27]; leftward triangles: 35%—1995–1996 [26]; downward triangles: 40%—1995–1996 [25], 40%—1995–1996 [5] (rhombuses), 45%—1995–1997 [26] (solid circles); rightward triangles: all the data with sum of gamma ray energies greater than 5 TeV [51]—1995–1999 [38,51]; stars: full data—1995-1999 [4]. The dotted line shows $(\beta_p{:}\beta_{\mathrm{He}}{:}\beta_{\mathrm{CNO}}{:}\beta_{\mathrm{NeMgSi}}{:}\beta_{\mathrm{Fe}} = 1.8{:}1.68{:}1.5{:}1.5{:}1.5)$ based on [6,9]. The solid line shows $(\beta_p{:}\beta_{\mathrm{He}}{:}\beta_{\mathrm{CNO}}{:}\beta_{\mathrm{NeMgSi}}{:}\beta_{\mathrm{Fe}} = 1.8{:}1.8{:}1.7{:}1.7{:}1.6)$ based on the RUNJOB assumption [5]. The dashed line shows $(\beta_p{:}\beta_{\mathrm{He}}{:}\beta_{\mathrm{CNO}}{:}\beta_{\mathrm{NeMgSi}}{:}\beta_{\mathrm{Fe}} = 2.79{:}2.81{:}2.80{:}2.83{:}2.62)$ based on the best fit to the data set from [5] (see Table XI, the first line for each element). The dash-dotted line shows the best fit to the data set from [25]: $(\beta_p{:}\beta_{\mathrm{He}}{:}\beta_{\mathrm{CNO}}{:}\beta_{\mathrm{NeMgSi}}{:}\beta_{\mathrm{Fe}} = 2.80{:}2.89{:}2.82{:}2.82{:}2.66)$ (see Table XI, the first line for each element). The filled area is taken from [5]. For clarity most of the error bars were omitted.

IV. DISCUSSION AND CONCLUSIONS

Although RUNJOB presented an interesting opportunity to look into the energy region which has been studied by other experiments, the attempt to claim that this observation is matching the expectations "of the shock acceleration process in supernova remnants" [4] is hardly reliable. In our present analysis we report on what we have learned, based on experimental data as they were presented and published. We can confirm that during ten successful balloon flights there was detected a high energy "particle" with primary energy ~1 PeV. We conclude that the results on energy spectra and intensities reported by RUNJOB could be significantly affected by the specific methods used in the RUNJOB analysis. We conclude that the probability to observe the reported energy spectra of protons in the energy region 8–500 TeV and helium in the energy region 2.5–75 TeV/n by eight chambers [5] during exposition 578.5 h [5] is practically zero. As a result, the RUNJOB data on helium as well as proton are not in disagreement with the assumption that the systematic differences in the methods of the RUNJOB analysis could result in apparent normalization differences with other experiments [5].

We do not dispute that further direct cosmic ray observations are essential. To discriminate among different models at a finer level will require more precise estimates of the power indices (i.e. significant increase of statistics) or a larger number of independent measurements with similar precision. Nevertheless, the RUNJOB experiment helps us to build the knowledge to generate the next set of hypotheses and experiments.

ACKNOWLEDGMENTS

V. K. would like to thank Professor Y.Fujimoto for many years of creative and productive collaboration, Professor K. Kondo and Professor S. Torii for the opportunity to work at the premises of the Advanced Research Institute for Science and Engineering, Waseda University during some stages of the preparation of this work, to Professor M. I. Panasyuk (Skobeltsyn Institute of Nuclear Physics, Moscow State University) for his long term interest in the RUNJOB experiment. Very sincere thanks (V. K.) to the staff and authorities of Waseda University, Aoyama Gakuin University, Hirosaki State University, Institute for Cosmic Ray Research of Tokyo University, and the National Diet Library (Kokuritsu Kokkai Toshokan) for the opportunity to work at their facilities, and for their kindness, cooperation, and practical help. We express our gratitude to the late Professor N. L. Grigorov (Skobeltsyn Institute of Nuclear Physics, Moscow State University), who honestly and courageously helped us to understand many mistakes and inconsistencies contained in a large variety of presentations. T. S. would like to express sincere thanks to Professor S. Kitayama of Rikkyo University for useful discussions. The authors are grateful to I. Asakura

and Y. Kumano for interesting communications and exchange of ideas. The authors wish to thank the anonymous referees for advice, valuable suggestions, and comments. We respect the great efforts of Russia and Japan in realization of the RUNJOB experiment.

APPENDIX A: FLIGHT INFORMATION

RUNJOB stated that the total exposure of 1995–1996 ''amounts to 231.5 m^2 h''. Table 1 from [5] showed that ''flight duration'' was ''578.5 h.'' The total exposure of 0.4 m^2 area for 578.5 h would result in 231.4 m^2 h. We found some inconsistencies in flight descriptions.

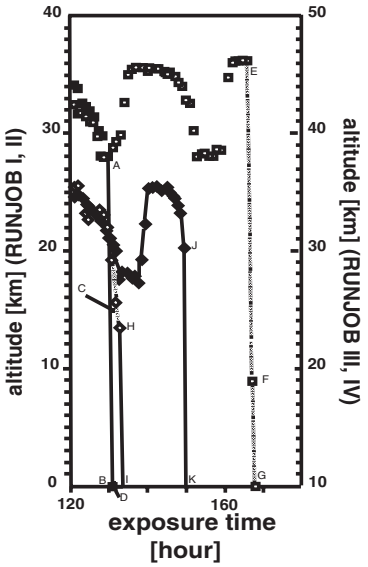

FIG. 10. The fragment of altitude profiles of four balloons. Solid squares: RUNJOB I, open squares: RUNJOB II, open rhombuses—RUNJOB III, solid rhombuses—RUNJOB IV. Estimations are made on the basis of data from [5,26,27,49]. RUNJOB collaboration stressed impressively stable trajectories of four balloons, as well as remarkable altitude fluctuations due to the ''day-night effect'' [5]. Using the RUNJOB reports and these statements, we can estimate the position of the termination point (TM), the last measurement point before touchdown (LP), and the touchdown point (TD). TM points in different flights are shown by characters A, J, E, LP points—C, H, F, and TD points—B, D, I, K, G. We found figures [26,27] which showed a slightly different profile at the final stage of RUNJOB I (points C, D). We noted that the figure caption read ''exposure time 130 h,'' while the touchdown point was shown at ~132 h (see Fig. 11). Original profiles of RUNJOB III and RUNJOB IV were shown as continuous lines only (no points). Both lines started at the altitude 0 at the beginning of the flight. While RUNJOB III abruptly ended at the altitude of ~23 km, the end of the RUNJOB IV line was almost approaching zero altitude at ~147.5 h [26,27]. The extrapolation of RUNJOB III flight until the touchdown (point I) was originally shown in [49] with caption ''the total exposure time 134 h.'' Points C and D are based on figures from [26,27], points A and B—on Fig. 2 from [5].

According to [29], ''the exposure time was 130 h for the first flight and 168 h for the second.'' Describing the same flights, [5] showed that flight duration was ''130 h'' for the first flight and ''167 h'' for the second flight. It seems that the words ''flight duration,'' ''exposure time,'' and ''total exposure time'' were used interchangeably [26,27,29,49]. Flight duration was estimated by RUNJOB with an accuracy of 0.5 h in [5]. Let us define the flight sequence, i.e. order of the different operations of the flight, as follows: launch, ascension, floating, flight termination, touchdown. Then, the term flight duration, or ''flight time'' means the elapsed time from the moment of launch until the moment the apparatus comes to rest at the end of the flight. The exposure time would be the amount of time a material is irradiated during flight time, since the passive emulsion chambers are always sensitive. It is obvious that one can consider some other definitions to estimate the exposure time: for instance, it can be ''at float time'' [9], ''flight time from launch until the terminate command,'' etc. Table 1 from [5] shows flight duration without clarification on what this duration means. Figure 10 shows the fragment of the RUNJOB I-IV flight profiles based on data from [5,26,27,49]. The RUNJOB plot [5] shows altitude versus time, from launch until touchdown. RUNJOB collaboration stressed ''impressively stable'' trajectories of four balloons, as well as ''remarkable'' altitude fluctuations

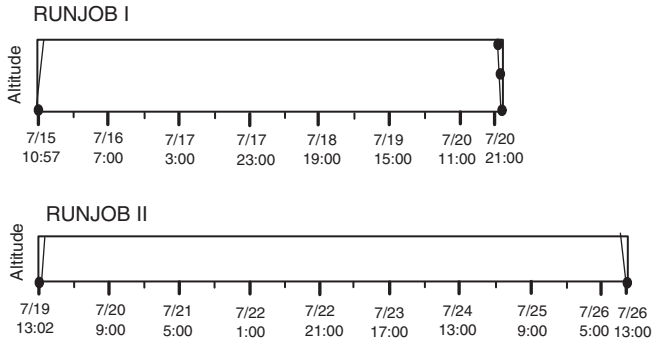

FIG. 11. Illustration of the timeline fragment for RUNJOB I and RUNJOB II. Data are based on figures from [26,27]. Solid circles with thin lines illustrate the position of experimental points at the beginning and at the end of flight. There were three experimental points between 130 h and 132 h in RUNJOB I (see points A, C, and D in our Fig. 10). The figure captions stated [26,27] that for RUNJOB I ''the total exposure time = 130 hours,'' and for RUNJOB II ''total exposure time = 168 hours.'' Major ticks on the x axis were shown with increment 20 hours, and minor ticks—10 hours. The last experimental point of RUNJOB I was placed at ~132 h (the period of time elapsed between 7/15 − 10:57 and 7/20 − 21:00 is 130 h 3 min, and there is an extra time of ~2 h between 7/20 − 21:00 and the experimental point) for RUNJOB I, and at ~168 h for RUNJOB II (the period of time elapsed between 7/19 − 13:02 and 7/26 − 13:00). Other figures on RUNJOB I from [5,26,27] showed just two points (A and B in our Fig. 10), with the caption ''the total exposure time = 130.5 h.''

TABLE XII. The final stage of RUNJOB flights in 1995–1996. Estimations are made on the basis of RUNJOB figures from [5,26,27,49]. It is important to notice that RUNJOB IV data in Fig. 2 from [5] were shifted in relation to the starting point ($t = 0$ h). In case of RUNJOB III and RUNJOB IV the total flight time is based on extrapolation [26,49] (the experimental points are missing at the touchdown level in Figure 2 from [5]).

Flight	Last point before landing, h (This work)	Flight termination, h (This work)	Touchdown time, h (This work)	Flight duration (exposure time), h RUNJOB [5]
1	<131[a]	~ 130	>130[a]	130.0[b]
2	~ 166	~ 166	~ 168	167.0[c]
3	~ 132	<132[d]	$>=134$[e]	134.0
4	<147[d]	>145 [e]	~ 147.5[f]	147.5

[a]Using [5,26,27]. See also Fig. 11.
[b]According to [29], the exposure time was 130 h. See also Table XIII.
[c]According to [29], the exposure time was 168 h. See also Table XIII.
[d]Taking into account altitude profile pattern due to impressively stable trajectories of four balloons, as well as remarkable altitude fluctuations due to the day-night effect [5].
[e]Using the extrapolation of RUNJOB III flight until the touchdown (point I), which was shown in [49] with caption the total exposure time 134 h, as well as earlier figures from [26,27].
[f]Early figures of the RUNJOB IV altitude profile showed a line (not scattered points) starting from the launch (zero altitude) until almost touchdown moment (close to zero altitude).

due to the day-night effect [5]. Using this information and assuming that points show measurement points, we can estimate the position of the ''termination point,'' the ''last point of measurement,'' and the ''touchdown point'' (see Fig. 10 and Table XII). For instance, the touchdown point of RUNJOB I was shown beyond the ~ 130 h mark in [5]. The early figures from [26,27] indicated that the total flight time of RUNJOB I could be even ~ 132 h (see Fig. 11). Tables with flight performance information [26,28] used Japanese word ''kaishuujikoku'' for the description of different flights. This word can be translated as ''recovery time, collection time, withdrawal time.'' While one can argue that a couple of hours can be regarded as being so negligible that it would not make any difference, we believe that for scientific evaluation one must apply similar criteria for different flights.

APPENDIX B: STEP-BY-STEP ALGORITHM

Here we describe our step-by-step algorithm, which can easily be implemented on a computer. The method computes a number of the expected primary particles in a given primary energy range, detected by a chamber with the detection efficiency ξ exposed during the $S\Omega T$ period to the primary flux dI/dE at the effective altitude t.

As an example we use here the numerical data related, for instance, to the detection of protons in RUNJOB I flight.

(1) We fix the input parameters: the chamber area S (0.4 m^2), the exposition period T ($130.0 \times 60.0 \times 60.0 = 468\,000.0$ seconds), the efficient altitude $t = 11.6$ g/cm^2, the efficient solid angle $\Omega = 2.88$, the attenuation length $\Lambda = 110$ g/cm^2, and the energy threshold $E_{\rm th} = 8$ TeV.
(2) We calculate the attenuation factor $e^{-t/\Lambda} = e^{-11.6/110.0}$.
(3) We generate a random sample A (of size 400) from a normal distribution with mean (22 600) and standard deviation (1300). Statistical software STATPLUS 2008 was used for this purpose.
(4) We generate a random sample B (of size 400) from a normal distribution with mean (2.78) and standard deviation (0.05). Statistical software STATPLUS 2008 was used for this purpose.
(5) For each random number A_i and B_i taken from A and B (where $i = 1400$), we generate a data set of primary particles with $E \geq E_{\rm th}$ from a power-law distribution with a power-law exponent B_i.
(6) Using the detection efficiency ξ, we count the number of particles contained in each energy bin with width $dE = 0.01$ TeV in the energy region above $E_{\rm th}$.
(7) We count the number of particles in the energy bins with the energy partition (expressed in TeV) suggested by RUNJOB in paper [5]: (8:14:26:42:70:140:500:3000).
(8) As a result, we produce a data set of 400 runs for RUNJOB I flight.
(9) We use steps (1)–(7) to produce a data set of 400 runs for RUNJOB II flight.
(10) We sum up these two data sets for RUNJOB I and RUNJOB II in the corresponding energy bins [step (7)]. We assume that the resulting data set represents the runs for the flight of the year 1995.
(11) We repeat steps (1)–(10) to produce a data set of 400 runs for RUNJOB III and RUNJOB IV flights.
(12) We repeat step (10) for RUNJOB III and RUNJOB IV, producing a data set which represents the flights of the year 1996.
(13) We count the number of particles in the energy bins [step (7)] using $400 \times 400 = 160\,000$ combinations of the data sets created at steps (10) and (12).

TABLE XIII. Basic information on the successful RUNJOB flights [5,25–28]. One can note some inconsistencies between the flight duration estimated by RUNJOB and the period of time between the launch and the termination of flight (based on the same RUNJOB data). In the reports [26,28] RUNJOB used Japanese word ''kaishuujikoku'' for the description of different flights. This word can be translated as ''recovery time, collection time, withdrawal time.'' Thus, the reported time values can represent quite different conditions for different flights. Mark NA stands for ''not available.'' The sum of all the numbers in brackets is 1437.5 h. Taking into account the area 0.4 m^2, we get 575 m^2 h, the total exposure of these campaigns [4].

Flight	Year	Launch m/day − h: min (L)	Withdrawal time m/day − h: min (WT)	Time period h: min (WT)-(L)	Flight duration (exposure time), h RUNJOB
1	1995	07/15 − 10:57[a]	07/20 − 21:00[a]	130:03	129[b], (130.0)[c], 130[d], 130.5[b], 132[e]
2	1995	07/19 − 13:02[a]	07/26 − 11:00[a]	165:58	(167.0)[c], 167 [b], 168[d]
3	1996	07/17 − 11:00[f]	07/23 − 01:00[f]	134:00	(134.0)[c], (134)[b], 145[g]
		07/17 − 09:00[a]	07/23 − 08:30[a]	143:30	
4	1996	07/18 − 13:00[a]	07/24 − 14:50[a]	145:50	(147.5)[c], 148[b], 162[g]
		07/18 − 12:00[f]	07/24 − 15:30[f]	147:30	
5	1997	07/09 − 12:15[a]	07/15 − 11:00[a]	142:45[h]	(139.5)[c], 140[b]
6	1997	07/11 − 14:15[a]	07/17 − NA[h]	NA[h]	(139.5)[c], 140[b]
8	1999	07/08 − 14:00[a]	07/14 − 11:30[a]	141:30	(141)[a]
9	1999	07/12 − 13:00[a]	07/18 − 14:30[a]	145:30	(145)[a]
10	1999	07/13 − 13:10[a]	07/19 − 17:10[a]	148:00	(148)[a]
11	1999	07/14 − 13:15[a]	07/20 − 16:00[a]	146:45	(146)[a]

[a][26,28].
[b][26,49].
[c][5,25,26,28].
[d][26,29].
[e]Using experimental point in figure from [26,27].
[f][26].
[g]These estimations [26] could be due to incorrect reading of the original altitude profile figure [26], where experimental data were shifted in respect to the point $t = 0$.
[h]We did not find any flight profile figures for RUNJOB V and VI.

(14) We calculate a mean and standard deviation in each energy bin for the data set of $400 \times 400 = 160\,000$ runs produced at step (13).

In our simulation set (PR-1) (see section ''Simulation'') we use different sets of A and B samples for different flights (RUNJOB I, RUNJOB II, RUNJOB III, RUNJOB IV). To compare the dependence of the chi-squared values on exposure time and effective altitude of observation [the simulation set (PR-2)], we used the same sets of A and B for corresponding flights.

[1] E. S. Seo, XIV ISVHECRI, Weihai, China, http://isvhecri2006.ihep.ac.cn/, 2006.
[2] T. Shibata, Report No. ICRR-REPORT-343-95-9, 1995.
[3] A calorimeter-type emulsion chamber is a detector that consists of many layers of x-ray films, nuclear emulsion plates, and other light or heavy materials plates. Most particles enter the calorimeter and initiate a shower, and the particles' energy is deposited in the calorimeter.
[4] V. A. Derbina *et al.* (RUNJOB Collaboration), Astrophys. J. **628**, L41 (2005).
[5] A. V. Apanasenko *et al.* (RUNJOB Collaboration), Astropart. Phys. **16**, 13 (2001).
[6] K. Asakimori *et al.* (JACEE Collaboration), Astrophys. J. **502**, 278 (1998).
[7] These slopes were obtained if RUNJOB focused ''on data given by RUNJOB and CRN alone ….'' The CRN stays for Cosmic Ray Nuclei experiment on Spacelab 2 (1985). See [52] for details.
[8] M. Hareyama *et al.* (RUNJOB Collaboration), J. Phys. Conf. Ser. **47**, 106 (2006).
[9] Y. Takahashi (JACEE Collaboration), Nucl. Phys. B, Proc. Suppl. **60**, 83 (1998).
[10] V. Zatsepin *et al.*, in *Proceedings of the XXIII ICRC*, edited by D. A. Leahy, R. B. Hicks, and D. Venkatesan (World Scientific, Calgary, Alberta, Canada, 1993), Vol. 2, pp. 13–16.
[11] K. Kobayakawa, Y. S. Honda, and T. Samura, Phys. Rev. D **66**, 083004 (2002).

[12] K. Kasahara *et al.*, Phys. Rev. D **66**, 052004 (2002).
[13] S. K. Gupta *et al.*, Phys. Rev. D **68**, 052005 (2003).
[14] M. Honda, T. Kajita, K. Kasahara, and S. Midorikawa, Phys. Rev. D **70**, 043008 (2004).
[15] T. Sanuki, M. Honda, T. Kajita, K. Kasahara, and S. Midorikawa, Phys. Rev. D **75**, 043005 (2007).
[16] F. A. Aharonian *et al.*, Phys. Rev. D **75**, 042004 (2007).
[17] V. Kopenkin, Y. Fujimoto, and T. Sinzi, Phys. Rev. D **68**, 052007 (2003).
[18] V. Kopenkin and Y. Fujimoto, Phys. Rev. D **73**, 082001 (2006).
[19] N. L. Grigorov (unpublished).
[20] V. Kopenkin (unpublished).
[21] V. Kopenkin and Y. Fujimoto, in *Proceedings of the 29th International Cosmic Ray Conference, Pune, India, 2005*, edited by B. S. Acharya, S. Gupta, P. Jagadeesan, A. Jain, S. Karthikeyan, S. Morris, and S. Tonwar (Tata Institute of Fundamental Research, Mumbai, 2005), Vol. 3, pp. 37–40.
[22] V. Kopenkin and Y. Fujimoto, Astron. Astrophys. **466**, 1211 (2007).
[23] One of us (V. K.) was listed as a coauthor of Ref. [4]. In spite of being a member of the RUNJOB collaboration at the time the paper was published, (V. K.) did not see the final manuscript before its publication nor the actual raw data upon which the manuscript was apparently based, Refs. [53–55], which were a complete surprise too.
[24] The RUNJOB conclusions on primary spectra did not differ significantly between so-called ''full'' data and 40% of data.
[25] A. V. Apanasenko *et al.* (RUNJOB Collaboration), Report No. ICRR-REPORT-459-2000-3, 2000.
[26] H. Nanjo, *Report on Japanese-Russian Collaboration Balloon Experiment in 1996–1999* (Hirosaki University, Japan, 2000), p. 296 (in Japanese).
[27] H. Nanjo, *Report on Japanese-Russian Collaboration Balloon Experiment in 1996–1997* (Hirosaki University, Japan, 1998), p. 204 (in Japanese).
[28] H. Nanjo, *Report on Japanese-Russian Collaboration Balloon Experiment in 1999–2001* (Hirosaki University, Japan, 2002), p. 141 (in Japanese).
[29] E. Kamioka *et al.* (RUNJOB Collaboration), Adv. Space Res. **26**, 1839 (2000).
[30] A. V. Apanasenko *et al.* (RUNJOB Collaboration), in Proceedings of the 22rd International Symposium on Space Technology and Science (22nd ISTS), Morioka, Japan, 2000, ISTS 2000-k-28.
[31] The $C_{k\gamma}^{-1}$ for the target interaction events were reported by JACEE as $\sim$0.265 for protons, and $\sim$0.265 for helium [9]. The conversion factor $C_{k\gamma}$ for typical elements (proton, helium, CNO, NeMgSi, iron) were similar for RUNJOB and JACEE. Slight differences arise due to the different chamber structure.
[32] A. V. Apanasenko *et al.* (RUNJOB Collaboration), Institute of Space and Astronautical Science (ISAS) Report, Special edition, No. 37, pp. 113–148 (1998), in Japanese.
[33] V. I. Galkin *et al.*, Report No. INPJ MSU 2002-1-685, 2002, p. 12.
[34] Another example of the detection efficiency (as a function of ΣE_γ) was presented in [25,32].
[35] For instance, in 2003 there was a graphical presentation of ''all data'' with shower energy ''above 5 TeV'' [37,38]. There are obvious differences between [37,38]. Apparently one paper [37] was based on the draft version submitted to the conference, and the other one [38] on the data made public during the conference. Then, so-called ''full'' data [4] might consist of all showers ''above 5 TeV'' from [38] and showers below 5 TeV. The numerical value of the lower threshold in this case is not clear and was not explicitly mentioned.
[36] A. A. Watson and A. W. Wolfendale, in *Astrophysical Aspects of the Most Energetic Cosmic Rays*, edited by M. Nagano and F. Takahara (World Scientific, Singapore, 1993), Vol. 403, pp. 13–16.
[37] M. Furukawa *et al.* (RUNJOB Collaboration), in *Proceedings of the 28th International Cosmic Ray Conference, Tsukuba, Japan*, edited by T. Kajita, Y. Asaoka, A. Kawachi, Y. Matsubara, and M. Sasaki (Universal Academy Press, Tokyo, 2003), Vol. 4, pp. 1877–1880.
[38] R. Battiston, in Proceedings of the 28th International Cosmic Ray Conference, Tsukuba, Japan (Ref. [37]), pp. 229–249, URL http://www-rccn.icrr.u-tokyo.ac.jp/icrc2003/talks/Rapporteur-Battiston.pdf.
[39] E. S. Pearson and H. O. Hartley, in *Biometrica Tables for Statisticians* (Cambridge University Press, Cambridge, England, 1966), 3rd ed., Vol. 1, p. 267.
[40] Y. Kawamura *et al.*, Phys. Rev. D **40**, 729 (1989).
[41] M. Ichimura *et al.*, Phys. Rev. D **48**, 1949 (1993).
[42] V. Zatsepin, in *Proceedings of the XXIII ICRC*, edited by D. A. Leahy, R. B. Hicks, and D. Venkatesan (World Scientific, Calgary, Alberta, Canada, 1993), Vol. 5, pp. 439–446.
[43] N. L. Grigorov, in *12th ICRC Hobart, Tasmania, 1971*, edited by A. G. Fenton and K. B. Fenton (University Tasmania Press, Hobart, Tasmania, 1971), Vol. 5, p. 1760.
[44] V. Kopenkin and Y. Fujimoto, Phys. Rev. D **71**, 023001 (2005).
[45] T. W. Kirkman, Statistics to Use, http://www.physics.csbsju.edu/stats/, 2007.
[46] K. Yoshida *et al.*, Phys. Rev. D **74**, 083511 (2006).
[47] N. L. Grigorov and E. D. Tolstaya, in *Proceedings of the 26th International Cosmic Ray Conference, Salt Lake City, Utah*, edited by D. Kieda, M. Salamon, and B. Dingus (University of Utah, Salt Lake City, 1999), Vol. 3, pp. 183–186.
[48] V. I. Galkin *et al.* (RUNJOB Collaboration), in *Proceedings of the XXIX All-Russia Conference on Cosmic Rays* [Izv. Ross. Akad. Nauk, Ser. Fiz. 71, 509 (2007)] (in Russian).
[49] A. V. Apanasenko *et al.* (RUNJOB Collaboration), in Proceedings of the 26th International Cosmic Ray Conference, Salt Lake City, Utah (Ref. [47]), pp. 163–166.
[50] M. Furukawa *et al.* (RUNJOB Collaboration), in Proceedings of the 28th International Cosmic Ray Conference, Tsukuba, Japan (Ref. [37]), pp. 1837–1840.
[51] M. Furukawa *et al.* (RUNJOB Collaboration), in Proceedings of the 28th International Cosmic Ray Conference, Tsukuba, Japan (Ref. [37]), pp. 1885–1888.
[52] S. P. Swordy *et al.*, Astrophys. J. **403**, 658 (1993).
[53] M. Hareyama *et al.* (RUNJOB Collaboration), in Proceedings of the 29th International Cosmic Ray

Conference, Pune, India, 2005 (Ref. [21]), pp. 17–20.
[54] M. Ichimura *et al.* (RUNJOB Collaboration), in Proceedings of the 29th International Cosmic Ray Conference, Pune, India, 2005 (Ref. [21]), pp. 21–24.
[55] L. G. Sveshnikova *et al.* (RUNJOB Collaboration), in Proceedings of the 29th International Cosmic Ray Conference, Pune, India, 2005 (Ref. [21]), pp. 49–52.